Low levels of soluble CD1d protein alters NKT cell function in patients with rheumatoid arthritis

SEIJI SEGAWA, DAISUKE GOTO, YOHEI YOSHIGA, TAICHI HAYASHI, ISAO MATSUMOTO, SATOSHI ITO and TAKAYUKI SUMIDA

Division of Clinical Immunology, Doctoral Program in Clinical Sciences, Graduate School of Comprehensive Human Sciences, University of Tsukuba, Japan

Received April 6, 2009; Accepted May 15, 2009

DOI: 10.3892/ijmm_00000256

Abstract. CD1d molecules on the cell surface play a critical role in the presentation of glycolipid antigens to natural killer T (NKT) cells. We previously showed that the human CD1d gene has 8 splice variants, one of which is a soluble form lacking the ß2-m and transmembrane domains. This study focused on soluble CD1d (sCD1d) by generating recombinant sCD1d proteins and assaying them in plasma using a newly established ELISA method. The amount of sCD1d proteins in plasma was significantly decreased in rheumatoid arthritis (RA) patients (55.2±13.3 years, mean ±SD) compared with healthy donors (31.2±7.4 years). Plasma sCD1d protein levels correlated with the number of NKT cells (TCR Vα24$^+$ Vß11$^+$ CD3$^+$) in peripheral blood mononuclear cells (r^2=0.061). Furthermore, sCD1d proteins induced IFN-γ production from NKT cells, but neither IL-4 nor IL-10. These findings suggest that the low plasma levels of sCD1d protein in RA patients reduce the number and thus activation of peripheral NKT cells. It is therefore hypothesized that sCD1d stimulates NKT cells and low plasma sCD1d levels in RA reflect a pathogenic mechanism associated with a decrease in NKT cells.

Correspondence to: Professor Takayuki Sumida, Division of Clinical Immunology, Doctoral Program in Clinical Sciences, Graduate School of Comprehensive Human Sciences, University of Tsukuba, 1-1-1, Tennoudai, Tsukuba, Ibaraki, 305-8575, Japan
E-mail: tsumida@md.tsukuba.ac.jp

Abbreviations: APC, antigen-presenting cell; α-GalCer, α-galactosylceramide; CIA, collagen-induced arthritis; ELISA, enzyme-linked immunosorbent assay; FBS, fetal bovine serum; IFN, interferon; IL, interleukin; mAb, monoclonal antibody; MHC, major histocompatibility complex; NKT, natural killer T; PBS, phosphate-buffered saline; RA, rheumatoid arthritis; rh, recombinant human; sCD1d, soluble CD1d; SD, standard deviation; TCR, T cell receptor; Th, T helper; ß2-m, ß2-microglobulin

Key words: natural killer T cells, autoimmune disease, rheumatoid arthritis, CD1d, soluble CD1d, rheumatoid arthritis

Introduction

The CD1 family of molecules comprises nonpolymorphic major histocompatibility complex (MHC) class I-like proteins (1-3), characterized by a 43-49-kDa heavy chain in noncovalent association with a 12-kDa ß2-microglobulin (ß2-m) light chain. CD1 genes map to chromosome 1q22-23 (4) and are classified into two groups based on sequence homology, group 1 (CD1a, 1b, 1c, and 1e) and group 2 (CD1d) (5,6). Group 1 CD1 molecules mainly present lipid antigens to clonally diverse T cells to mediate adaptive immunity against a vast range of microbial lipid antigens. In contrast, CD1d (group 2) molecules are expressed on the surface of cortical thymocytes (7), B cells (8), dendritic cells (9-11), Langerhan's cells in the skin (12), and gastrointestinal epithelial cells (9,11). The soluble form of CD1d (sCD1d) presents glycolipid antigens to natural killer T (NKT) cells.

NKT cells express the surface marker, NKR-P1A (CD161), and a highly restricted T-cell antigen receptor (TCR) comprised of an invariant TCRα chain with a single rearrangement (TCR Vα14-Jα18 in mice, and TCR Vα24-Jα18 in humans) (13) coupled with TCRß chains with limited heterogeneity due to marked skewing of TCR Vß gene usage (mostly TCR Vß8.2 in mice and TCR Vß11 in humans) (14). NKT cells recognize glycosphingolipid α-galactosylceramide (α-GalCer), bind to CD1d, and respond by secreting a variety of cytokines, including Th1 cytokines such as IL-2 and IFN-γ, and Th2 cytokines such as IL-4 and IL-10 in humans or IL-17 in mice (15). This ability to potently modulate adaptive immunity upon stimulation of a restricted set of antigen-specific receptors, together with a lack of immunological memory, closely resembles the properties of cell types belonging to the innate immune system (16).

Human NKT cells are believed to regulate immune tolerance or autoimmunity (17). Indeed, the NKT cell number is selectively decreased in human autoimmune diseases, such as rheumatoid arthritis (RA), systemic sclerosis, systemic lupus erythematosus, Sjögren's syndrome, and type I diabetes mellitus (18-20).

We previously identified alternatively spliced variants of human CD1d mRNA in peripheral blood mononuclear cells (PBMCs) (21). Two of these, V1 and V2, were considered functional due to complete conservation of the antigen-binding site. V1 lacks exon 4 (ß2-m binding domain) of the CD1d gene, resulting in unstable antigen presentation, while V2 lacks both

exon 4 and 5 (transmembrane domain), resulting in sCD1d. The expression levels of sCD1d mRNA were significantly lower in RA patients than healthy donors, although there was no significant difference in the number of intact $CD1d^+$ cells in peripheral blood (22). The functional relevance of sCD1d protein, which is present in plasma, remains unclear. The present study was designed to determine the plasma sCD1d levels by developing a new two-sites enzyme-linked immunosorbent assay (ELISA) detection system. Preliminary testing with this method showed significantly low plasma sCD1d protein and sCD1d mRNA levels in PBMCs of RA patients compared with those of healthy donors. In addition, plasma levels of sCD1d protein correlated with the proportion of NKT cells among PBMCs. These findings implicate a role for sCD1d in stimulating NKT cell production. The relevant effects in RA are also discussed.

Materials and methods

Patients and healthy donors. We examined 52 patients with RA (age 55.2±13.3 years, mean ±SD) diagnosed according to the criteria of the American College of Rheumatology (ACR; formerly, the American Rheumatism Association). All patients and 40 disease-free healthy donors (31.2±7.4 years of age) were referred to the University of Tsukuba Hospital and gave their written consent for this study. The study was approved by the ethics committee of the university of Tsukuba Hospital.

Plasma and PBMC samples. The PBMCs of patients and healthy donors were isolated using Ficoll-Paque (GE Healthcare UK, Little Chalfont, UK) density-gradient centrifugation. The supernatant was recovered as plasma, and the pelleted PBMC fraction was ready for use after washing twice with phosphate-buffered saline (PBS).

Polyclonal antibody specific for sCD1d. Rabbits were injected every 2 weeks for a total of 5 times with sCD1d-specific C-terminal 14-mer (QDLWTSGSQDFSPG) peptides linked to a carrier protein (KLH). Whole blood was collected and the serum obtained.

Constructs and reagents. V1 CD1d and sCD1d cDNA were obtained from PBMCs as described previously (22). The PCR-products were subsequently digested with *Hind*III-*Not*I and cloned into pcDNA3.1 (Invitrogen, San Diego, CA), resulting in pcDNA3.1-sCD1d, -V1 CD1d, and -mock as a control. The cloned PCR-fragments were sequenced in both directions according to a standard protocol (ABI PRISM BigDye Terminator Cycle Sequencing Ready Reaction Kit) and analyzed using an ABI PRISM 310 Genetic Analyzer (Applied Biosystems, Framingham, PA).

Production and purification of soluble CD1d proteins. Cos-7 cells ($5x10^5$) were grown on 10-cm tissue culture dishes (TPP) in Dulbecco's modified Eagle's medium supplemented with 10% fetal bovine serum (BioWest, FL) and 1% penicillin/streptomycin (Invitrogen) at 37°C with 5% CO_2. Plasmid DNA was transfected into Cos-7 cells using FuGeneHD transfection reagents (Roche, Basel, Switzerland), and the cells were cultured for 24 h before rinsing in PBS and lysis in the following buffer, 50 mM Na_2PO_4, 300 mM NaCl, 0.5% NP-40, and 2 mM phenylmethylsulfonyl fluoride (PMSF), pH 7.4. The supernatant obtained after centrifugation at 10,000 x g was used as purification sample.

Proteins were then purified using HiTrap NHS-activated HP affinity columns (GE Healthcare) according to the instructions provided by the manufacturer. The FLAG column prepared above was used for immunoaffinity purification of FLAG M2 antibody (Sigma, St. Louis, MO). The column was washed sequentially with start buffer (10 mM Tris-HCl, pH 7.5) and elution buffer (100 mM glycine, pH 2.5), and was finally equilibrated with start buffer. Purified samples were loaded onto the column. Bound proteins were eluted with 0.1 M glycine, pH 2.5, and the pH was brought to neutral by adding 0.1 volume of neutralizing buffer (1 M Tris-HCl, pH 8.0). After elution, the samples were concentrated and dialyzed against PBS using an Amicon Ultra with a 10-kDa cut-off (Millipore, Billerica, MA).

Immunoprecipitation and immunoblotting. sCD1d-transfected cells were lysed and subjected to immunoblotting (blot). Aliquots of the lysates were separated by SDS-polyacrylamide gel electrophoresis (SDS-PAGE) and transferred to membranes (Bio-Rad, Hercules, CA). The membranes were subjected to blotting with anti-FLAG antibodies. The culture supernatants of sCD1d-transfected cells were subjected to immunoprecipitation (IP) with anti-CD1d monoclonal antibodies followed by adsorption to protein G Sepharose (Pharmacia Biotech, Uppsala, Sweden). The precipitates were immunoblotted with anti-FLAG antibodies.

Specific ELISA assay systems for soluble CD1d. A two-sites ELISA assay was established to detect and measure sCD1d. Anti-human CD1d monoclonal antibody (mAb; 0.1 μg/ml, Santa Cruz Biotechnology, Santa Cruz, CA) in PBS was added to wells of a plate (Nunc, Roskilde, Denmark) and incubated overnight at 4°C. The wells were washed three times with a wash buffer (0.05% Tween-20 in PBS), and then blocked with commercial blocking buffer (Dainippon Sumitomo Seiyaku, Osaka, Japan) for 2 h at 37°C. We then added 100 μl of a plasma sample diluted 1:5 in PBS and incubated overnight at room temperature. After washing three times with wash buffer, 100 μl of anti-sCD1d polyclonal antibody (prepared in-house) diluted to 1:1,000 in PBS was added to each well and incubated for 4 h at 37°C. After washing three times with wash buffer, 100 μl of horseradish peroxidase (HRP)-labeled anti-rabbit antibody (Santa Cruz Biotechnology) diluted 1:3,000 in PBS, was added to each well, and incubated for 2 h at 37°C. After final washing (6 times) with the wash buffer, 100 μl of substrate (Pierce, Rockford, IL) was added to each well, and left for 90 min. The optical density (OD) of each well was measured at 405 nm using a microplate reader (Bio-Rad).

Staining and flow cytometry. Fluorescein isothiocyanate (FITC)-labeled anti-TCR Vα24 and phycoerythrin (PE)-labeled anti-TCR Vß11 monoclonal antibodies were purchased from Beckmann Coulter (Fullerton, CA). The allophycocyanin (APC)-conjugated anti-CD3 monoclonal antibody (mAb) was obtained from BioLegend (San Diego, CA). The frequency of invariant NKT cells was estimated using three-color anti-TCR

Vα24/anti-TCR Vß11/anti-CD3 staining. The stained cells were analyzed on a CyAn ADP (DAKO, Glostrup, Denmark) and data were processed using Summit4.3 (DAKO).

Preparation of antigen presenting cells. PBMCs were isolated using Ficoll-Paque (GE Bioscience) density gradient centrifugation, and CD14+ monocytes were harvested from the PBMCs using a MACS system (Miltenyi Biotec, Bergisch Gladbach, Germany). The CD14+ monocytes were cultured for 6 days in complete RPMI 1640 (supplemented with 10% heat-inactivated fetal bovine serum (BioWest), 1% penicillin/streptomycin, 10 mM N-2-hydroxyetylpiperazine-N'-ethane-sulphonic acid (HEPES)-NaOH, 0.1 mM minimum essential medium (MEM) nonessential amino acids, 1 mM sodium pyruvate, and 5.5 μM 2-mercaptoethanol (Invitrogen) in the presence of 50 ng/ml recombinant human granulocyte-monocyte colony-stimulating factor (GM-CSF) and 100 ng/ml recombinant human IL-4 (R&D Systems, Minneapolis, IL) to obtain human monocyte-derived dendritic cells (Mo-DCs).

Expansion and sorting of TCR Vα24+ Vß11+ NKT cells. PBMCs were isolated using Ficoll-Paque (GE Bioscience) density gradient centrifugation and cultured with 100 ng/ml α-galactosylceramide (α-GalCer, Krin Brewery, Gunma, Japan) and 100 ng/ml recombinant human IL-2 (rhIL-2, MBL, Woburn, MA) at a density of 10^6 cells/ml complete RPMI 1640. After 7 days, cells were restimulated with α-GalCer-pulsed Mo-DCs and co-cultured with 100 ng/ml rhIL-2. On day 7 after restimulation, Vα24+ cells were isolated using a MACS system (Miltenyi Biotec). These isolated cells were then again restimulated with α-GalCer pulsed Mo-DCs and co-cultured with 100 ng/ml rhIL-2. The expanded NKT cells were stained with FITC-labeled anti-TCR Vα24 mAb, PE-labeled anti-TCR Vß11 mAb and APC-labeled anti-CD3 mAb. The CD3+, Vα24+, Vß11+ lymphocyte-gated cells were sorted on a MoFlo cell sorter (DAKO).

Stimulation of TCR Vα24+ Vß11+ NKT cells by plate-bound CD1d dimer or sCD1d protein. Multiwell Plates were coated with CD1d dimer XI (1 μg in 100 μl PBS/well), purified sCD1d protein, or mock protein for 16 h. After washing with PBS, α-GalCer was added (0.1 ng/μl in PBS/well) and incubated at 37°C for another 24 h. NKT cells were then added to the wells and cytokine production analyzed after a further 72 h.

Measurement of cytokines. The cytokine levels in the culture supernatants were evaluated by ELISA (R&D Systems).

Statistical analysis. Data are expressed as a median and mean ±SD. Data were analyzed using a statistical software package (Stat View 5.0, SAS Institute, NC). Differences between groups were examined for statistical significance using the Mann-Whitney U-test and Spearman's rank correlation. A P-value <0.05 denoted the presence of a statistically significant difference.

Results

Soluble CD1ds are expressed intra- and extracellularly. We reported previously the expression of sCD1d mRNA in PBMCs

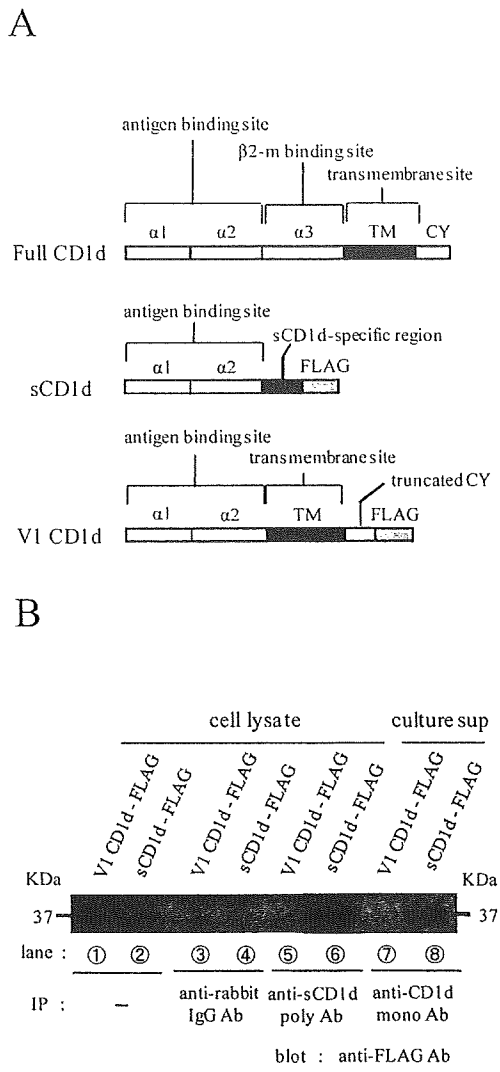

Figure 1. Expression of recombinant variant CD1d proteins. (A) Recombinant proteins of sCD1d and V1 CD1d were cloned into expression vectors, with FLAG tags expressed at the C-terminus for purification and detection. (B) Cos-7 cells were transfected to express V1 CD1d and sCD1d. After incubation for 24 h, cells were harvested to analyze the expression using anti-sCD1d polyclonal antibodies. We performed immunoprecipitation (IP) and immunoblotting (blot) analysis as indicated. Lanes 1-2, positive control; lanes 3-4, negative control; lanes 5-6, anti-sCD1d polyclonal antibodies specific for sCD1d protein; lanes 7-8. The secreted recombinant sCD1d was also detected in the Cos-7 cell culture supernatant. Only sCD1d molecules were detected and not other CD1d variant (V1) proteins.

(21). sCD1ds are characterized by defective alignment of the ß2-m binding and transmembrane domains, compared to other family members (21) (Fig. 1A). To examine whether sCD1d proteins are secreted, we expressed recombinant FLAG-tagged sCD1d in Cos-7 cells. Culture supernatants were immunoprecipitated using anti-CD1d monoclonal antibodies, and bound proteins detected by immunoblotting with anti-FLAG antibodies (Fig. 1B). The sCD1d protein was present in culture supernatants, although the V1 was not detected. V1 CD1d is considered insoluble, because the transmembrane domain unique to CD1d is completely conserved (Fig. 1A). These results indicate that sCD1d protein is secreted extracellularly and it is likely that the same mechanism applies *in vivo*.

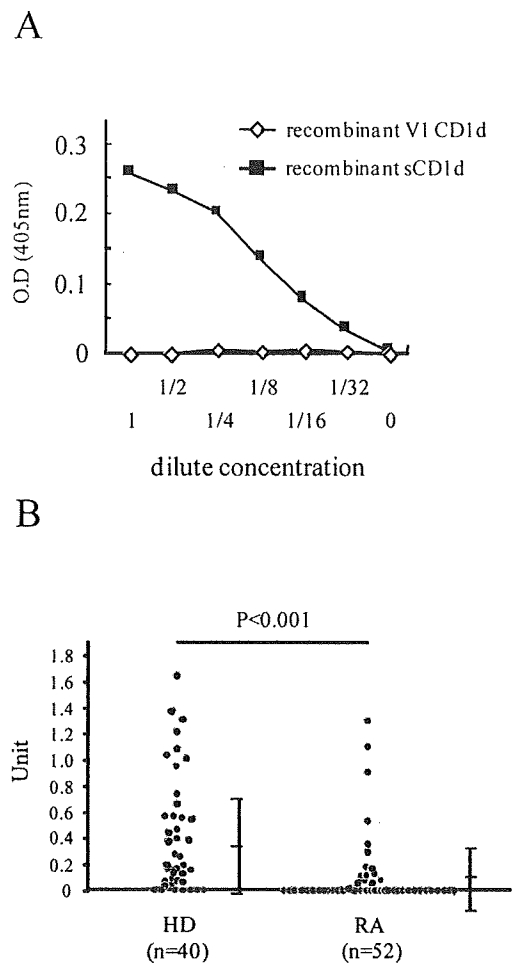

Figure 2. Establishment of sCD1d-specific ELISA using anti-CD1d monoclonal and anti-sCD1d polyclonal antibodies to reveal low sCD1d proteins in RA patients. (A) Purified recombinant V1 CD1d and sCD1d proteins as specifically measured by the developed ELISA system. (B) The levels of sCD1d proteins in plasma of healthy donors (n=40) and RA patients (n=52) determined by the sCD1d-specific ELISA. The level of secreted sCD1d protein in RA patients (0.10±0.29 U/ml) was significantly lower than in healthy donors (0.39±0.42 U/ml). Each point represents the sCD1d ratio (unit) from a specific healthy control. Comparison of median between different groups was performed using the Mann-Whitney U test.

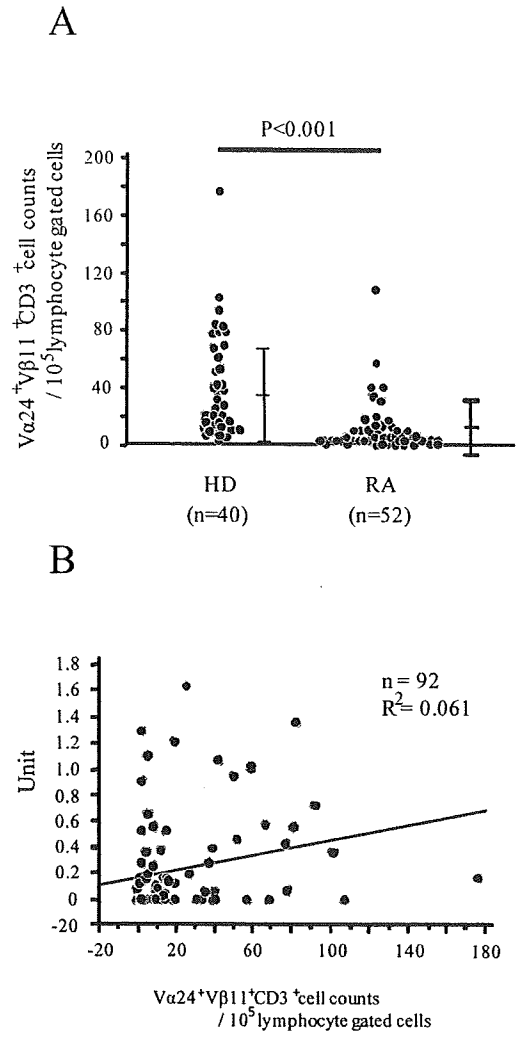

Figure 3. Correlation between sCD1d protein in plasma and NKT cells in PBMCs. (A) NKT cells among PBMCs from healthy donors (n=40) and RA patients (n=52) were stained with monoclonal antibodies, FITC-labeled anti-TCR Vα24 mAb, PE-labeled anti-TCR Vß11 mAb, and APC-labeled anti-CD3 mAb. The number of NKT cells in 10^5 PBMCs was counted. NKT cells were significantly fewer in number in RA patients (10.6±18.2 cells) compared with healthy donors (40.5±36.1 cells). Comparison of median values between different groups was performed using the Mann-Whitney U test. (B) Plasma sCD1d protein levels correlated with the number of NKT cells in PBMCs (r^2=0.061). Comparison of median values between different groups was performed using Spearman's rank correlation.

Patients with RA have low plasma levels of sCD1d. To examine the levels of sCD1d proteins in the peripheral blood of patients with RA, we established the sCD1d-specific ELISA. The specificity of sCD1d binding was confirmed by recombinant sCD1d and V1 CD1d proteins (Fig. 2A). Preliminary experiments indicated that detection of sCD1d protein was more sensitive in plasma compared with serum (data not shown). Therefore, plasma samples from 52 RA patients and 40 healthy donors were tested. The sCD1d protein concentrations in plasma samples of RA patients (0.10±0.29 U/ml) were significantly lower than those of healthy controls (0.39±0.42 U/ml) (Fig. 2B). Though there was a significant difference in age between healthy donors and RA patients, we confirmed age had no influence on sCD1d expression in plasma (data not shown).

Plasma levels of sCD1d protein correlated with number of TCR Vα24+ Vβ11+ NKT cells. We also determined the proportion of NKT cells in PBMCs from the same set of plasma samples. RA patients had significantly fewer NKT cells (10.6±18.2 cells) than healthy controls (40.5±36.1 cells) (Fig. 3A). Interestingly, the plasma levels of sCD1d protein correlated significantly with the number of NKT cells in peripheral blood, as we reported previously (20) (Fig. 3B). This result suggests that sCD1d stimulates and activates NKT cells.

α-GalCer-bound sCD1d protein stimulates TCR Vα24+ Vβ11+ NKT cells. To determine the functional significance of sCD1d, NKT cells were incubated with sCD1d and cytokine production was measured. NKT cells from healthy donors were expanded using α-GalCer (Fig. 4A), and then sorted to isolate TCR Vα24+ Vß11+ NKT. These cells were then cultured in the presence of recombinant sCD1d protein plus α-GalCer, or plate-bound CD1d dimer XI plus α-GalCer as a control. After incubation for 72 h, secreted IFN-γ, IL-4 and IL-10 were

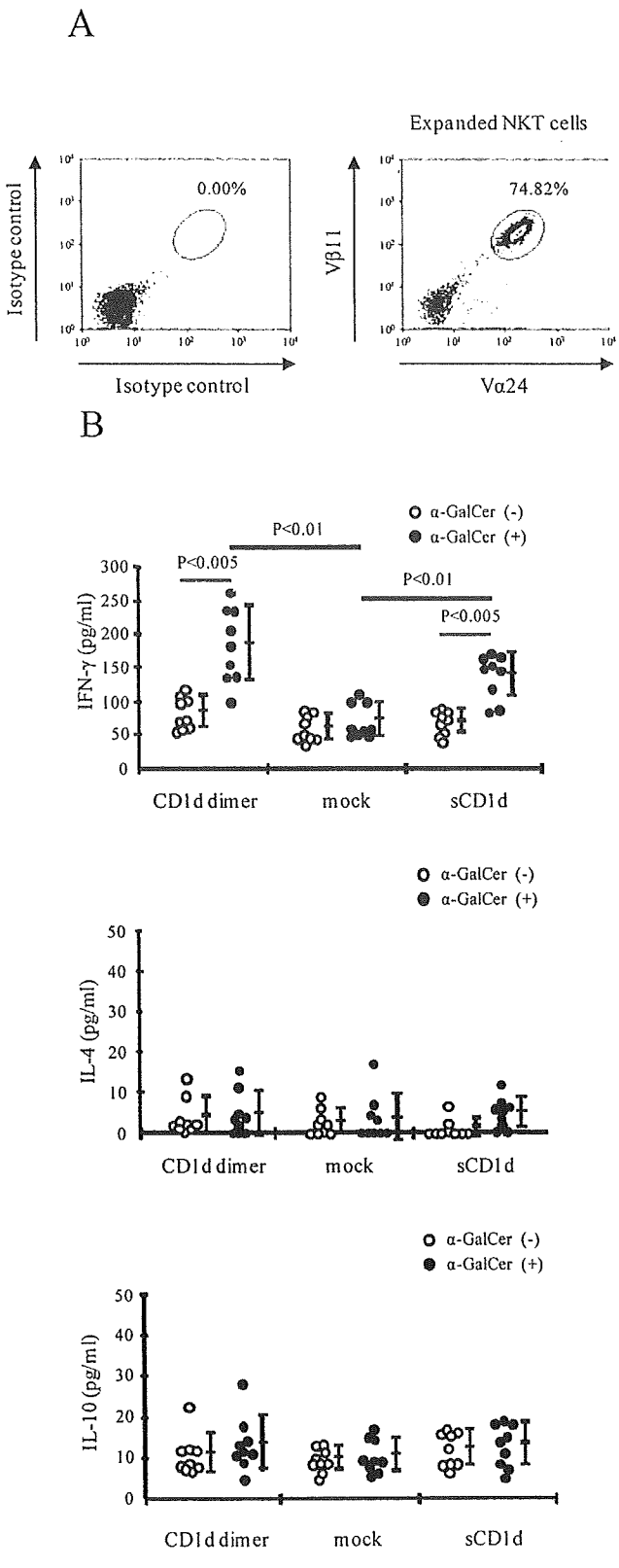

Figure 4. Stimulation of Vα24+ Vß11+ NKT cells by sCD1d protein. (A) NKT cells from healthy donors were expanded as described in Materials and methods. Expanded NKT cells were stained with FITC-labeled anti-TCR Vα24 mAb, PE-labeled anti-TCR Vß11 mAb, APC-labeled anti-CD3 mAb, and FITC + PE-labeled isotype control Ab. Values are the percentage of cells relative to the gated CD3+ cell population. (B) NKT cells from healthy donors (n=9) were expanded and sorted (CD3+Vα24+ Vß11+). Sorted NKT cells were stimulated by plate-bound CD1d dimer XI, mock proteins, or sCD1d proteins with (•) and without (○) α-GalCer. IFN-γ, IL-4 and IL-10 were assayed in culture supernatants after 72 h. The secretion of IFN-γ was increased in the presence of sCD1d plus α-GalCer. Comparison of median values between different groups was performed using Student's t-test.

measured by ELISA. Secretion of IFN-γ from NKT cells increased with sCD1d plus α-GalCer (138.5±33.1 pg/ml) compared with mock protein plus α-GalCer (73.53±17.36 pg/ml) ($p<0.01$) (Fig. 4B), whereas that of IL-4 and IL-10 did not (Fig. 4B).

Discussion

Human NKT cells are thought to regulate immune tolerance or autoimmunity (17), with autoimmune disease patients showing significantly fewer NKT cells than healthy controls (18-20). However, the mechanisms by which these cell numbers are reduced remain unknown. The current study reveals significantly less sCD1d protein in the plasma of a group of RA patients compared with healthy donors. Considering the demonstrated relationship between sCD1d proteins and NKT cell numbers, these findings implicate a role for sCD1d in NKT cell activation.

Overexpression experiments demonstrated that the sCD1d protein was indeed secreted into the extracellular medium, even if without the ß2-m binding domain. In support of this, others have shown CD1d expression on intestinal epithelial cells in ß2-m-deficient mice (23).

The results obtained here also imply that sCD1d stimulates NKT cells, by combining NKT cells with recombinant sCD1d proteins and measuring cytokine production. NKT cells were stimulated to produce IFN-γ in the presence of sCD1d mixed with lipids antigens (α-GalCer). Previous studies (24,25) demonstrated soluble HLA class I molecules (sHLAs) in sera from patients with RA, SLE, and multiple sclerosis. These soluble HLAs acted by binding to TCR on alloreactive T cells (26). It is therefore possible that sCD1d binds to TCR on NKT cells *in vivo*, stimulated by a natural ligand, and thus activates the NKT cells.

In an arthritis mouse model, Chiba *et al* (27) showed that *in vivo* activation of NKT cells using α-GalCer inhibited collagen-induced arthritis (CIA). Another study (28) also demonstrated NKT cell activation in α-GalCer-aggravated joint inflammation. The amount of lipid antigens present in these experiments were insufficient to suppress inflammations in the models used. The current study, however, strongly supports that the lipid antigens activated NKT cells not only via intact CD1d, but also via sCD1d *in vivo*. We speculate that the RA patients had decreased sCD1d protein secreted, resulting in reduced NKT cell numbers and thus activation.

Acknowledgements

We thank Dr F.G. Issa for a critical reading of the manuscript. This study was supported in part by the Grant-in-Aid for Scientific Research by the Japan Society for the Promotion of Science and the Japanese Ministry of Health, Labour and Welfare.

References

1. Martin LH, Calabi F and Milstein C: Isolation of CD1 genes: A family of major histocompatibility complex-related differentiation antigens. Proc Natl Acad Sci USA 83: 9154-9158, 1996.
2. Martin LH, Calabi F, Lefebvre FA, *et al*: Structure and expression of the human thymocyte antigens CD1a, CD1b, and CD1c. Proc Natl Acad Sci USA 84: 9189-9193, 1987.

3. Balk SP, Bleicher PA and Terhost C: Isolation and characterization of cDNA and gene coding for a fourth CD1 molecule. Proc Natl Acad Sci USA 86: 252-256, 1989.
4. Albertson DG, Fishpool R, Sherrington P, *et al*: Sensitive and high resolution in situ hybridization to human chromosomes using biotin labeled probes: Assignment of the human thymocyte CD1 antigen genes to chromosome 1. EMBO J 7: 2801-2805, 1988.
5. Calabi F, Jarvis JM, Martin L, *et al*: Two classes of CD1 genes. Eur J Immunol 19: 285-292, 1989.
6. Procelli SA and Modlin RL: The CD1 system: antigen-presenting molecules for T cell recognition of lipids and glycolipids. Annu Rev Immunol 17: 297-329, 1999.
7. Amiot M, Bernard A, Raynal B, *et al*: Heterogeneity of the first cluster of differentiation: Characterization and epitopic mapping of three CD1 molecules on normal human thymus cells. J Immunol 136: 1752-1758, 1986.
8. Small TN, Knowles RW, Keever C, *et al*: M241 (CD1) expression on B lymphocytes. J Immunol 138: 2864-2868, 1987.
9. Delia D, Cattoreti G, Polli N, *et al*: CD1c but neither CD1a nor CD1b molecules are expressed on normal, activated, and malignant human B cells: Identification of a new B-cell subset. Blood 72: 241-247, 1988.
10. Blumberg RS, Terhorst C, Bleicher P, *et al*: Expression of a nonpolymorphic MHC class I-like molecule, CD1D, by human intestinal epithelial cells. J Immunol 147: 2518-2524, 1991.
11. Meunier L, Gonzalez-Romos A and Cooper KD: Heterogeneous populations of class II MHC$^+$ cells in human dermal cell suspensions. Identification of a small subset responsible for potent dermal antigen-presenting cell activity with features analogous to Langerhans cells. J Immunol 151: 4067-4080, 1993.
12. Canchis PW, Bhan AK, Landau SB, *et al*: Tissue distribution of the nonpolymorphic major histocompatibility complex class I-like molecule, CD1d. Immunology 80: 561-565, 1993.
13. Lantz O and Bendelac A: An invariant T cell receptor alpha chain is used by a unique subset of major histocompatibility complex class I-specific CD4$^+$ and CD4-8$^-$ T cells in mice and humans. J Exp Med 180: 1097-1106, 1994.
14. Yu KO, Im JS, Molano A, *et al*: Modulation of CD1d-restricted NKT cell responses by using N-acyl variants of alpha-galactosylceramide. Proc Natl Acad Sci USA 102: 3383-3388, 2005.
15. Yoshiga Y, Goto D, Segawa S, *et al*: Invariant NKT cells produce IL-17 through IL-23-dependent and -independent pathways with potential modulation of Th17 response in collagen-induced arthritis. Int J Mol Med 22: 369-374, 2008.
16. Coppieters K, Dewint P, Van Beneden K, *et al*: NKT cells: manipulable managers of joint inflammation. Rheumatology 46: 565-571, 2007.
17. Sandberg JK, Fast NM and Palacios EH: Selective loss of innate CD4$^+$ Vα24 natural killer T cells in human immunodeficiency virus infection. J Virol 76: 7528-7534, 2002.
18. Sumida T, Sakamoto A, Murata H, *et al*: Selective reduction of T cells bearing invariant V alpha 24J alpha Q antigen receptor in patients with systemic sclerosis. J Exp Med 182: 1163-1168, 1995.
19. Wilson SB, Kent SC and Patton KT: Extreme Th1 bias of invariant Vα24JαQ T cells in type 1 diabetes. Nature 391: 177-181, 1998.
20. Kojo S, Adachi Y, Keino H, *et al*: Dysfunction of T cell receptor AV24AJ18$^+$BV11$^+$ double negative regulatory natural killer T cells in autoimmune disease. Arthritis Rheum 44: 1127-1138, 2001.
21. Kojo S, Adachi Y, Tsutsumi A and Sumida T: Alternative splicing forms of the human CD1d gene in mononuclear cells. Biochem Biophys Res Commun 276: 107-111, 2000.
22. Kojo S, Tsutsumi A, Goto D and Sumida T: Low expression levels of soluble CD1d gene in patients with rheumatoid arthritis. J Rheumatol 30: 2524-2528, 2003.
23. Kim HS, Garcia J and Blumberg RS: Biochemical characterization of CD1d expression in the absence of beta2-microgloblin. J Biol Chem 274: 9289-9295, 1999.
24. Tsuchiya N, Shiota M, Yamaguchi A and Ito K: Elevated serum level of soluble HLA class I antigens in patients with systemic lupus erythematosis. Arthritis Rheum 39: 792-796, 1997.
25. Filaci G, Contini P and Brenci S: Soluble HLA class I and class II molecule levels in serum and cerebrospinal fluid of multiple sclerosis patients. Hum Immunol 54: 54-62, 1997.
26. Zavazava N and Kronke M: Soluble HLA class I molecules induce apoptosis in alloreactive cytotoxic T lymphocyte. Nat Med 2: 1005-1010, 1996.
27. Chiba A, Oki S, Miyamoto K, Hashimoto H, *et al*: Suppression of collagen-induced arthritis by natural killer T cell activation with OCH, a sphingosine-truncated analog of galactosylceramide. Arthritis Rheum 50: 305-313, 2004.
28. Kim HY, Kim HJ, Min HS, *et al*: NKT cells promote antibody-induced joint inflammation by suppressing transforming growth factor 1 production. J Exp Med 201: 41-47, 2005.

Mod Rheumatol (2009) 19:229–234
DOI 10.1007/s10165-009-0162-4

ORIGINAL ARTICLE

Efficacy of mizoribine pulse therapy in patients with rheumatoid arthritis who show a reduced or insufficient response to infliximab

Masanobu Horikoshi · Satoshi Ito · Mizue Ishikawa · Naoto Umeda · Yuya Kondo · Hiroto Tsuboi · Taichi Hayashi · Daisuke Goto · Isao Matsumoto · Takayuki Sumida

Received: 10 November 2008 / Accepted: 13 February 2009 / Published online: 27 March 2009

Abstract The efficacy of infliximab, a chimeric antibody against tumor necrosis factor-α used to treat patients with rheumatoid arthritis (RA), tends to decrease as patients develop human antichimeric antibody against infliximab (HACA). The clinical study reported here was designed to evaluate the efficacy of mizoribine (MZR) pulse therapy in patients who show a reduced or insufficient response to infliximab. Ten RA patients who had active arthritis despite infliximab therapy were treated with MZR pulse therapy at a dose of 100 mg MZR and methotrexate (MTX) and the disease activity assessed at baseline and at weeks 4–8, 12–16, and 20–24. The dose was increased to 150 mg in those patients who showed an insufficient response to MZR. The mean 28-joint disease activity score (DAS28) at weeks 12–16 and 20–24 of therapy was significantly lower than that at baseline. A moderate or good European League against Rheumatism (EULAR) response was achieved in seven patients (70%) at weeks 12–16 and in five patients (50%) at weeks 20–24. The dose of 150 mg MZR was effective in one of the three patients who showed an insufficient response to pulse therapy with 100 mg MZR. Based on these results, we propose that MZR pulse therapy should be attempted before the patient is switched to other biologics.

Keywords Infliximab · Mizoribine · Rheumatoid arthritis

M. Horikoshi · S. Ito (✉) · M. Ishikawa · N. Umeda · Y. Kondo · H. Tsuboi · T. Hayashi · D. Goto · I. Matsumoto · T. Sumida
Division of Clinical Immunology, Doctoral Program in Clinical Sciences, Graduate School of Comprehensive Human Science, University of Tsukuba, Tsukuba, Japan
e-mail: s-ito@md.tsukuba.ac.jp

Introduction

Infliximab is a chimeric anti-tumor necrosis factor-alpha (TNF-α) monoclonal antibody that has proven effective in patients with rheumatoid arthritis (RA) [1–3]. In Japan, mizoribine (MZR; 4-carbamoyl-1-b-D-ribofuranosylimidazolium) is used as an immunosuppressive agent in patients undergoing renal transplantation and receiving treatment for RA and lupus nephritis in Japan. This drug inhibits inosine monophosphate dehydrogenase, a rate-limiting enzyme in the de novo pathway of nucleic acid synthesis, thereby inhibiting lymphocyte proliferation [4, 5]. Mizoribine, which is usually used at a daily dose of 75–150 mg administered in three separate doses, is known for its low rate of side effects [6], but it has been considered comparatively less effective than other disease-modifying antirheumatic drugs (DMARDs) in patients with RA. A correlation between the peak MZR blood concentration and clinical response to the therapy has been observed in patients with lupus nephritis [7]. It has also been recently shown that a drug therapeutic regimen consisting of 100–150 mg MZR once daily is more effective than the three divided doses because the achieved blood concentration was higher with the former [8]. Mizoribine pulse therapy has also been found to be effective in patients with RA who show an inadequate effect of methotrexate (MTX) [9–11]. In the case of MZR pulse therapy, patients receive MZR on one or two days of the week combined with MTX. The basis of this combination therapy is that MZR inhibits the synthesis of purines and MTX inhibits primarily the synthesis of pyrimidines; consequently, both drugs together inhibit the de novo pathway of nuclei acid synthesis. As such, the combined use of these two drugs is considered to inhibit lymphocyte proliferation more effectively than either used solely (monotherapy) [12].

Tokuda et al. [9] reported the efficacy of MZR pulse therapy as additional therapy for nine patients who showed an insufficient effect of MTX. Five of the nine patients responded to the combined MZR pulse + MTX drug therapeutic regimen within 20 weeks. Kohriyama et al. [10] and Murai et al. [11] also reported the efficacy of MZR pulse therapy as additional therapy in patients showing an inadequate effect of MTX.

An important problem associated with the use of infliximab in therapeutic drug regimens is that its efficacy often decreases during prolonged treatment. In Japan, the approved dose of infliximab is up to 3 mg/kg, or 200 mg/body, and that of MTX is up to 8 mg/week. Insufficient doses of these drugs may contribute to a decrease in the clinical efficacy of infliximab. The objective of this clinical study was to evaluate the efficacy of MZR pulse therapy in patients who show reduced or insufficient response to infliximab.

Patients and methods

Background of the patients

Ten RA patients treated with infliximab between 2005 and 2008 at Tsukuba University Hospital were enrolled in this study. Of these, eight showed a reduced response to infliximab (=high disease activity despite the clinical response to infliximab by week 30 of treatment), and two showed an insufficient response to infliximab (=no clinical response to infliximab during the 30-week treatment period). All ten patients fulfilled the American College of Rheumatology criteria for RA revised in 1987 [13]. They all had active arthritis as defined by the 28-joint disease activity score (DAS28) >3.2 at study entry, with the exception of one patient who wanted to receive MZR therapy despite a DAS28 of 3.0. The mean ± standard deviation (SD) age of the patients was 50.3 ± 12.8 years, the mean ± SD disease duration was 6.5 ± 6.2 years, and the mean ± SD DAS28 using erythrocyte sedimentation rate (ESR; DAS28-ESR) was 5.0 ± 1.5.

All patients were concomitantly receiving MTX, 6–8 mg/week. The doses of concomitant prednisolone and DMARDs, including MTX, were not increased during the last 3 months prior to entry in the study.

Study protocol and clinical response

This study was approved by the ethical committee of our hospital. Informed consent was obtained before the study. Patients first received 100 mg of MZR together with MTX. The patients received 300 mg MZR on the first two days of the week: 200 mg MZR on the first day in two divided doses and 100 mg MZR in one dose on the second day (Fig. 1). At the time of each infusion of infliximab, the swollen joint count (SJC), tender joint count (TJC), visual analogue score (VAS), ESR, and DAS28 were recorded. Five of the ten patients were started on MZR pulse therapy between the infusions of infliximab. We therefore we assessed the patients' DAS28 at baseline and after 12–16 weeks, 20–24 weeks and, thereafter, every 8 weeks.

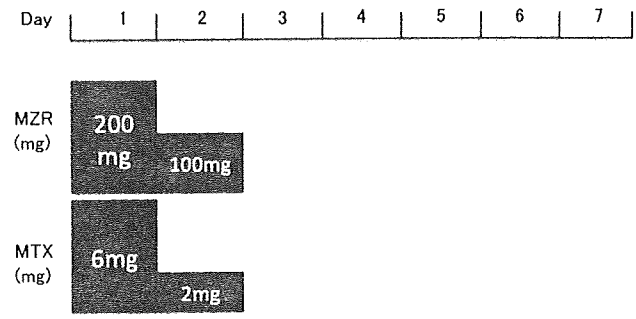

Fig. 1 The schedule of mizoribine (*MZR*) pulse therapy, consisting of combination drug therapy with 100 mg methotrexate (*MTX*). Total drug therapeutic program was 8 mg/week of MTX

Statistical analysis

We analyzed data using the Student's *t* test to assess whether the changes in DAS28 and laboratory data from baseline during the course of the treatment were significant.

Results

The clinical socio-demographic and clinical characteristics of the patients, including previously administered DMARDs (as well as those drugs continued during the study), response to MZR pulse therapy [according to the EULAR (European League Against Rheumatism) response criteria at weeks 12–16, and weeks 20–24], response to infliximab (according to the EULAR response criteria at week 30), and change in the dose of prednisolone (PSL) between baseline and week 24, are shown in Table 1.

All of the patients were followed for more than 24 weeks. The MZR pulse therapy was well tolerated, and none of the patients discontinued the therapy. Seven patients (70%) had achieved a moderate or good EULAR response at weeks 12–16, and five patients (50%) had achieved a moderate or good EULAR response at weeks 20–24,.

The mean DAS28 decreased from 5.0 at baseline to 3.9 ($P = 0.047$) at week 16, and 4.1 ($P = 0.043$) at week 24 (Fig. 2). The mean C-reactive protein (CRP) and ESR levels decreased, although not significantly during MZR pulse therapy.

Table 1 Clinical and socio-demographic characteristics of the patient cohort

Case no.	Sex	Age (years)	Duration of RA (years)	Stage[a]	Previous DMARDs[b]	Response to IFX[c]	Baseline DAS28[d]	Response to MZR[e]/ DAS28 (weeks 12–16)	Response to MZR/ DAS28 (weeks 20–24)	Dose of predonisolone
1	M	64	8	II	SASP BC	Moderate	7.9	Good 3.0	Moderate 4.5	No change
2	F	48	4	III	SASP BC	Good	4.0	Good 2.5	Good 2.5	No change
3	F	32	2.5	II	SASP BC	Good	4.8	Moderate 4.2	No 4.7	No change
4	F	41	1.5	I	SASP BC	Moderate	6.9	No 7.3	No 7.3	8 → 3 mg
5	F	55	2.5	II	SASP BC	No	5.2	Moderate 4.2	Moderate 4.3	8 → 7 mg
6	M	29	20	IV	SASP BC D-PC	No	4.1	Moderate 3.4	No 4.2	No change
7	F	65	2	I	SASP BC	Moderate	3.0	No 3.1	No 2.8	No change
8	M	59	1	I	SASP	Good	3.8	Moderate 2.9	No 3.3	No change
9	F	50	11	IV	SASP BC GST	Good	4.2	No 3.9	Good 2.7	10 → 8 mg
10	M	60	12	II	BC	Moderate	5.6	Moderate 4.3	Moderate 5.0	No change

RA rheumatoid arthritis, *IFX* infliximab, *MZR* mizoribine

[a] Steinbrocker stage of radiographs

[b] Disease-modifying antirheumatic drugs, including drugs continued during the study. *SASP* salazosulfapyridine, *BC* bucillamine, *D-PC* D-penicillamine, *GST* gold sodium thiomalate

[c] EULAR (European League Against Rheumatism) response criteria, at week 30

[d] DAS28-ESR, 28-joint disease activity score based on erythrocyte sedimentation rate

[e] EULAR response criteria

Three patients showed insufficient or reduced response to MZR pulse therapy after 24 weeks; we therefore increased the dose of MZR up to 150 mg in these patients. One of these patients showed a favorable response to the higher dose (case 2). None of the patients had an adverse reaction to the higher dose, not even a minor infection, nor were there any abnormalities in the laboratory data. A complete blood count, including white blood cells, neutrophils, lymphocytes, hemoglobin, and platelet counts, demonstrated the absence of any significant changes that could be related to MZR pulse therapy (Table 2).

Two successful cases of MZR pulse therapy are described below in detail.

Case 1 was a 48-year-old woman who had been successfully treated with 10 mg/kg of infliximab during a clinical trial for 54 weeks. Her DAS28 had been less than 2.6 during the trial, but infliximab therapy was stopped after the eighth infusion because the trial was finished. Thereafter, her disease activity increased, (DAS28 3.7), and infliximab therapy was restarted at a dose of 2.6 mg/kg (the maximum approved dose is 200 mg and her body weight was 77 kg; therefore, she was administered 2.6 mg/kg infliximab). However, her disease activity did not decrease despite three additional infusions of infliximab. We therefore considered that 2.6 mg/kg infliximab had limited efficacy in this patient and added MZR pulse therapy at a dose of 100 mg together with MTX. By 4 weeks after the iniation of the MZR pulse thereapy, her DAS28 had decreased to 2.4. At week 20 on MZR pulse therapy, she achieved a good EULAR response (Fig. 3).

Case 2 was a 64-year-old man whose disease had been successfully controlled with infliximab, but who showed an increase of the disease activity while still on this drug. We therefore added MZR pulse therapy at a dose of 100 mg together with MTX 4 weeks before the 19th infusion of infliximab. Twenty weeks later, his DAS28 had decreased to 3.0 ,and he had achieved a good EULAR response. Thereafter, his disease activity was under control for over 24 weeks. At the time of the 25th infusion of infliximab, his DAS28 was 5.4, and his disease activity had increased again. We then increased the dose of MZR to 150 mg. Eight weeks later, his DAS28 had decreased to 3.5 (Fig. 4).

This second case suggests that increasing the dose of MZR may be effective. The clinical response to MZR pulse therapy was most clearly observed in cases 1 and 2, probably because infliximab showed some degree of efficacy in these patients. In case 4, although the patient's DAS28 did not decrease until week 24 of treatment, MZR pulse therapy was considered to be clinically effective because we were able to decrease the dose of PSL from 8 to 3 mg.

Discussion

In Japan, infliximab has been used to treat RA patients since 2003. Although it efficacy in Japanese RA patients was demonstrated in the RECONFIRM study [14], the results of this study also indicated that the clinical response to infliximab may decline after 30 weeks of drug therapy.

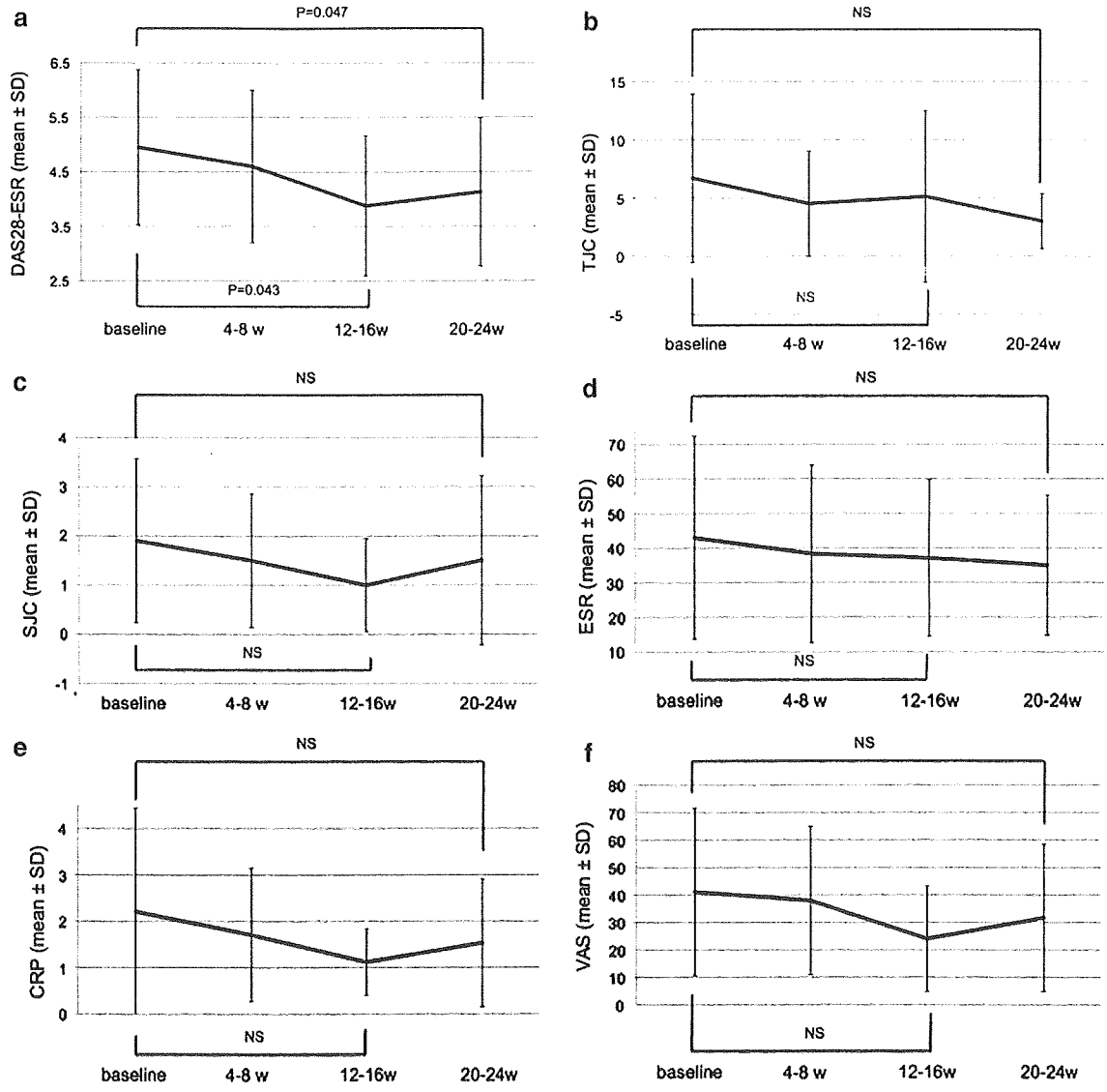

Fig. 2 **a** Changes in the 28-joint disease activity score (DAS28) from baseline and during the MZR pulse therapy regimen, at weeks 4–8, 12–16, and 20–24. The DAS28 significantly decreased at 12–16 weeks ($P = 0.047$) and at 20–24 weeks ($P = 0.043$). **b** Change in the tender joint count (*TJC*) at baseline and during therapy, at 4–8, 12–16, and 20–24 weeks. **c** Change in the swollen joint count (*SJC*) at baseline and during therapy, at 4–8, 12–16, and 20–24 weeks. **d** Change in the erythrocyte sedimentation rate (*ESR*) at baseline and during therapy, at 4–8, 12–16, and 20–24 weeks. **e** Change in the C-reactive protein (*CRP*) at baseline and during therapy, at 4–8, 12–16, and 20–24 weeks. **f** Change in the visual analog scale (*VAS*) at baseline and during therapy, at 4–8, 12–16, and 20–24 weeks. *NS* Not significant

This reduced effect of infliximab therapy in relation to the development of human antichimeric antibody against infliximab (HACA) has been reported in several studies [15, 16]. An increase of the dose of infliximab beyond 3 mg/kg (e.g., 5, 10 mg/kg) or the shortening of the interval between infliximab infusions (e.g., every 6 weeks) has proven to be effective in such cases [2, 17, 18]. However, these methods are not approved by the Japanese Ministry of Health, Labor and Welfare. Etanercept is another biological product available in Japan. Alternating anti-TNF therapies, such as switching between etanercept and infliximab, has been reported to be effective in patients who do not respond to their first anti-TNF drug [19, 20]. However, such switching of anti-TNF therapy was strictly limited in Japan because only two biologics were available when we started this study. Tocilizumab and adalimumab were approved in Japan in April 2008, thereby doubling the number of biologics that can be used to treat patients with RA (four); however, the choice of biologics is still limited because some patients refuse self-injection. In our opinion,

Table 2 Results of a complete blood count among the patient cohort at baseline and at 20–24 weeks after the initiation of MZR pulse therapy

Laboratory blood tests	Baseline	At weeks 20–24	*P*
WBC (/μl)	7410 ± 2100	7000 ± 1510	NS
Lymphocyte (/μl)	2050 ± 1690	1750 ± 1110	NS
Neutrocyte (/μl)	5030 ± 1870	4470 ± 940	NS
Hemoglobin (g/dl)	12.7 ± 1.1	12.6 ± 1.5	NS
Platelet count ($\times 10^4$/μl)	32.0 ± 8.0	33.3 ± 9.9	NS

Values are given as the mean ± standard deviation of white blood cell (WBC), lymphocyte, neutrocyte, hemoglobin, and platelet counts before (baseline) and 20–24 weeks after the initiation of MZR pulse therapy

NS not significant

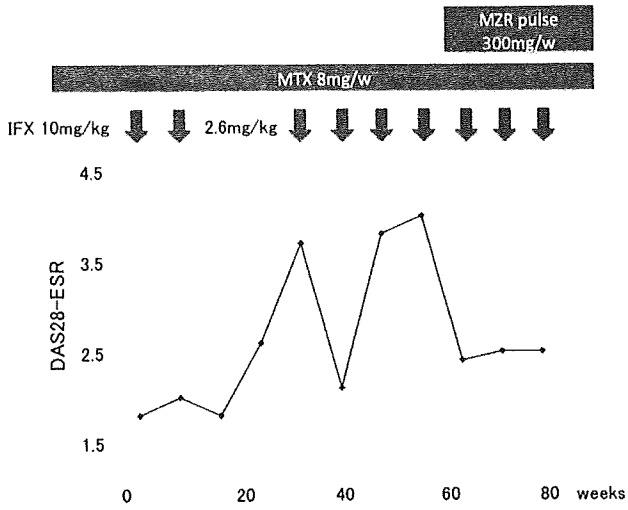

Fig. 3 Response to therapy by patient 1 (case 1). *IFX* Infliximab

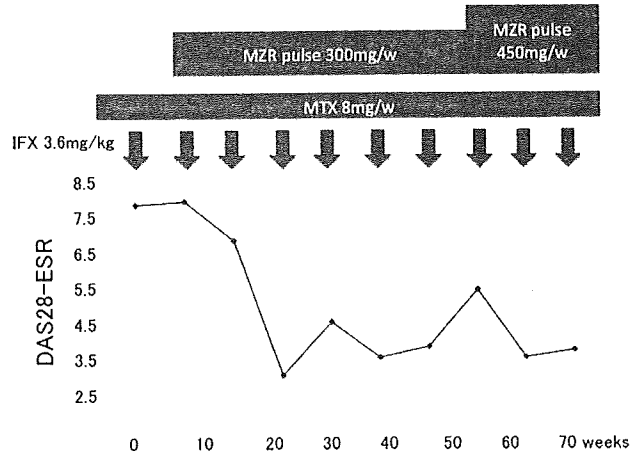

Fig. 4 Response to therapy by patient 2 (case 2)

it is better to use one biological agent as long as possible—and not a combination—because it is still unclear whether the other biologics decrease the effect.

The objective of this study was to evaluate the efficacy and safety of MZR pulse therapy in patients who showed a reduced or insufficient response to infliximab. We observed significant efficacy at weeks 12–16 and at weeks 20–24. The decrease in the number of patients who responded to the therapy at weeks 20–24 (relative to weeks 12–16) may suggest a decline in the response of our patients to MZR pulse therapy. In this situation, a higher dose of MZR combined with MTX may be effective, as shown in case 1. Further studies are needed to confirm the efficacy of the higher dose of MZR.

The response rate using MZR pulse therapy that we obtained in this study in patients who showed a reduced response to infliximab (70%; 7/10 patients with a moderate or good EULAR score) was higher than that reported in previous studies using MZR pulse therapy (16–50%) in patients who showed inadequate response to MTX (without infliximab) [9–11]. This difference in response rate suggests that MZR pulse therapy may have some additional effect other than that as a DMARD. Although we could not measure anti-infliximab antibody levels, it would appear that MZR pulse therapy administered concomitantly with infliximab, in addition to its effect as a DMARD, also inhibits HACA.

In conclusion, in our small study cohort of patients with RA, MZR pulse therapy proved to be effective in patients who showed a reduced response to infliximab. We suggest that, in cases where infliximab is ineffective, MZR pulse therapy should be attempted before the patient is switched to another biologic.

Conflict of interest statement None.

References

1. Maini R, St Clair EW, Breedveld F, et al. Infliximab (chimeric anti-tumour necrosis factor alpha monoclonal antibody) versus placebo in rheumatoid arthritis patients receiving concomitant methotrexate: a randomized phase III trial. Lancet. 1999;354: 1932–9.
2. Lipsky PE, van der Heijde DM, St Clair EW, et al. Infliximab and methotrexate in the treatment of rheumatoid arthritis. N Eng J Med. 2000;343:1594–602.
3. St Clair EW, van der Heijde DM, Smolen JS, et al. Combination of infliximab and methotrexate therapy for early rheumatoid arthritis. A randomized, controlled trial. Arthritis Rheum. 2004; 50:3432–43.
4. Ishikawa H. Mizoribine and mycophenolate mofetil. Curr Med Chem. 1999;6:575–97.
5. Koyama H, Tsuji M. Genetic and biochemical studies on the activation and cytotoxic mechanism of bredinin, a potent inhibitor of purine biosynthesis in mammalian cells. Biochem Pharmacol. 1983;32:3547–53.
6. Tanaka E, Inoue E, Kawaguchi Y, et al. Acceptability and usefulness of mizoribine in the management of rheumatoid arthritis in methotrexate-refractory patients and elderly patients, based on

analysis of data from a large-scale observational cohort study. Mod Rheumatol. 2006;16:214–9.
7. Kuroda T, Hirose S, Tanabe N, et al. Mizoribine therapy for patients with lupus nephritis: the association between peak mizoribine concentration and clinical efficacy. Mod Rheumatol. 2007;17:206–12.
8. Shida J, Shuto T, Tokito T, et al. Clinical investigation of efficacy by administration of mizoribine once a day for rheumatoid arthritis (in Japanese). Kyushu Riumachi. 2006;26:9–14.
9. Tokuda M, Dobashi H, Hiraishi M, et al. Effect of mizoribine pulse therapy on the disease activity of rheumatoid arithritis refractory to the treatment with methotrexate (in Japanese). Rheumatology. 1998;20:519–26.
10. Kohriyama K, Hiramatsu Y, Aoyama T, et al. Efficacy of combination pulse therapy with methotrexate and mizoribine for patients with rheumatoid arthritis showing escape phenomenon to low-dose methotrexate therapy (in Japanese). Rinsyo Riumachi. 2003;15:227–34.
11. Murai T, Arai K, Fujisawa J, et al. Evaluation of combination pulse therapy with methotrexate and mizoribine for patients with methotrexate-resistant rheumatoid arthritis (in Japanese). Jpn J Joint Dis (in press).
12. Nishimura K, Itoh K, Kuga Y, et al. Prevention of joint destruction in rheumatoid arthritis patients receiving combination methotrexate and mizoribine therapy: a two-year, multicenter open-comparison study to methotrexate monotherapy. Prog Med. 2006;26:2163–72.
13. Arnett FC, Edworthy SM, Bloch DA, et al. The American Rheumatism Association 1987 revised criteria for the classification of rheumatoid arthritis. Arthritis Rheum. 1988;31:3315–24.
14. Yamanaka H, Tanaka Y, Sekiguchi N, et al. Retrospective clinical study on the notable efficacy and related factors of infliximab therapy in a rheumatoid arthritis management group in Japan (RECONFIRM). Mod Rheumatol. 2007;17(2):178.
15. Gerrit JW, Marijin V, Willem L, et al. Development of antiinfliximab antibodies and relationship to clinical response in patients with rheumatoid arithritis. Arthritis Rheum. 2006;54:711–5.
16. van der Bijl AE, Breedveld FC, Antoni CE, et al. An open-label pilot study of the effectiveness of adalimumab in patients with rheumatoid arthritis and previous infliximab treatment: relationship to reasons for failure and anti-infliximab antibody status. Clin Rheumatol. 2008;27:1021–8.
17. St. Clair EW, Carrie LW, Adedigbo A, et al. The relationship of serum infliximab concentrations to clinical improvement in rheumatoid arthritis: results from ATTRACT, a multicenter, randomized, double-blind, placebo-controlled trial. Arthritis Rheum. 2002;46:1451–9.
18. Elisabeth H, Mikkel O, Jan P, et al. Do rheumatoid arthritis patients in clinical practice benefit from switching from infliximab to a second tumor necrosis factor alpha inhibitor? Ann Rheum Dis. 2007;66:1184–9.
19. Van Vollenhoven R, Harju A, Brannemark S, Klareskog L. Treatment with infliximab (Remicade) when etanercept (Enbrel) has failed or vice versa: data from the STURE registry showing that switching tumour necrosis factor α blockers can make sense. Ann Rheum Dis. 2003;62:1195–8.
20. Cohen G, Courvoisier N, Cohen JD, et al. The efficiency of switching from infliximab to etanercept and vice versa in patients with rheumatoid arthritis. Clin Exp Rheumatol. 2005;23:795–800.

PEDIATRIC AND DEVELOPMENTAL PATHOLOGY

The Official Journal of the Society for Pediatric Pathology and the Paediatric Pathology Society
Affiliated with the International Paediatric Pathology Association

Hydrops Fetalis Due to Agenesis of the Ductus Venosus: New Hepatic Histological Features

MAKOTO TAKEUCHI,[1,2*] MASAHIRO NAKAYAMA,[1] ARIHIRO TAMURA,[3] AND HIROYUKI KITAJIMA[3]

[1]Department of Pathology, Osaka Medical Center and Research Institute for Maternal and Child Health
[2]Department of Pathology, Ikeda Municipal Hospital
[3]Department of Neonatology, Osaka Medical Center and Research Institute for Maternal and Child Health

Pediatric and Developmental Pathology 12, 239–243, 2009
DOI: 10.2350/07-10-0363.1

Hydrops Fetalis Due to Agenesis of the Ductus Venosus: New Hepatic Histological Features

MAKOTO TAKEUCHI,[1,2*] MASAHIRO NAKAYAMA,[1] ARIHIRO TAMURA,[3] AND HIROYUKI KITAJIMA[3]

[1]Department of Pathology, Osaka Medical Center and Research Institute for Maternal and Child Health
[2]Department of Pathology, Ikeda Municipal Hospital
[3]Department of Neonatology, Osaka Medical Center and Research Institute for Maternal and Child Health

Received October 22, 2007; accepted November 9, 2008; published online December 12, 2008.

ABSTRACT

We describe the clinical course and autopsy findings of a male infant with hydrops fetalis due to agenesis of the ductus venosus. Fetal echocardiography at 27 weeks in gestation demonstrated hydrops fetalis due to unknown causes. The baby was born at 28 weeks in gestation by emergency caesarean section because of preeclampsia and progressive hydrop fetalis but died immediately at birth. The umbilical vein catheter ran an unusual course: left renal vein and inferior vena cava were opacified after postmortem injection of radiopaque dye into the umbilical vein. The autopsy demonstrated agenesis of the ductus venosus without extrahepatic umbilical venous drainage. The type without extrahepatic venous drainage is rare but shows a favorable outcome in general. However, our findings illustrate that in addition to sinusoidal dilatation, some cases may induce significant medial hypertrophy of portal veins, leading to hydrops fetalis and neonatal demise.

Key words: agenesis of the ductus venosus, extrahepatic umbilical venous drainage, hepatic pathology, hydrops fetalis, portal hypertension

INTRODUCTION

The ductus venosus (DV) links the persisting left umbilical vein and portal vein directly to the inferior vena cava (IVC). It allows a portion of the well-oxygenated blood coming from the placenta to bypass the high-resistance hepatic vascular network. The high-velocity jet coming from the DV preferentially circulates blood flow toward the foramen ovale, providing optimal oxygenation to the fetal brain, and a sphincter mechanism of the DV protects the fetal heart from excessive blood flow from the placenta [1,2]. Agenesis of the DV collapses fetal circulation and causes various hemodynamic consequences [3–10]. We present a case of hydrops fetalis due to agenesis of the ductus venosus associated with unique hepatic microscopic findings.

*Corresponding author, e-mail: makoto-takeuchi@hosp.ikeda.osaka.jp

CASE REPORT

The mother was a 35-year-old gravida 4, para 3 Japanese woman. The pregnancy had been uneventful until 23 weeks in gestation. The fetus developed hydrops fetalis at 27 weeks' gestation. A 2806-g male was born at 28 weeks' gestation by emergency caesarean section because of preeclampsia and progressive hydrop fetalis. Apgar scores were 2 and 2 at 1 and 5 minutes, respectively. The infant was resuscitated immediately. However, his clinical condition deteriorated further despite intensive and cardiac support. Laboratory evaluation revealed severe hypoproteinemia (1.9 mg/dl) without liver dysfunction. Karyotype analysis was normal (46,XY). At this time the umbilical vein catheter was observed to follow an unusual and strange course on an X-ray (Fig. 1A). The baby died 19 hours later. Left renal vein and IVC were detected when we took an X-ray of the whole body after postmortem injection of a radiopaque dye from the umbilical vein catheter (Fig. 1B).

At autopsy, the baby had bilateral pleural effusion, marked pericardial effusion, ascites, and anasarca characteristic of hydrops fetalis. The DV was absent (Fig. 2). Neither remnant nor string in the fissure of the ligamentum venosum was detected; therefore, there was not premature obstruction of the DV. The umbilical vein drained into the portal vein and had no communication with IVC. We could detect the umbilical vein catheter first in the umbilical vein, then in the portal vein, the gastric coronary vein, and the gastrorenal collaterals, and finally in the left renal vein. Thus, all the placental venous flow drained exclusively into the portal vein which might induce portal hypertension and abnormal vascular collateral anatomy. Therefore, we could conclude that the course of collateral vessels was due to portal hypertension. The liver was of normal size but was congestive. Microscopically, the sinusoids and central vein of the liver were extensively and diffusely dilated (Fig. 3A). Extramedually hematopoiesis was prominent.

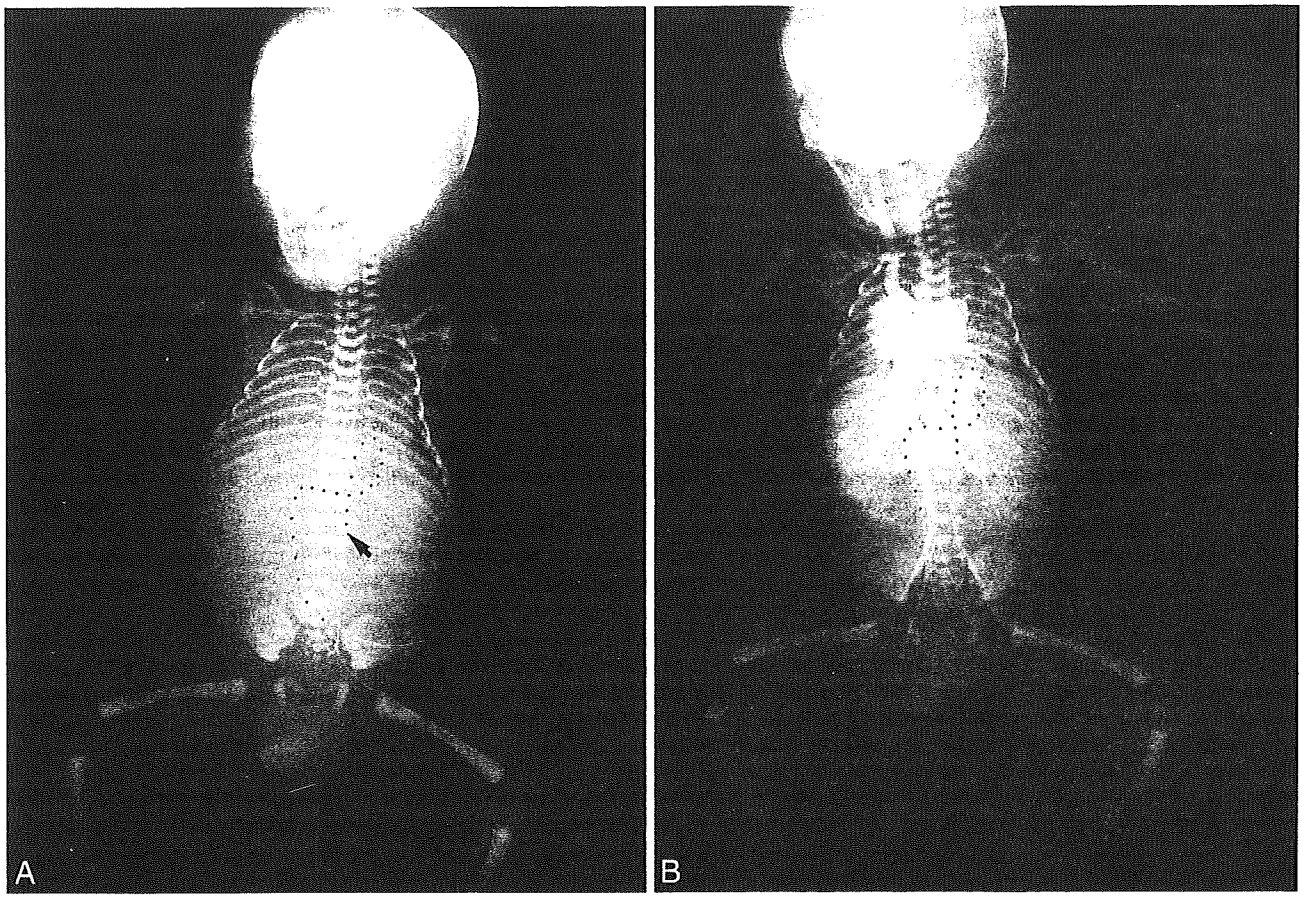

Figure 1. Total body X-ray examination. **A.** The umbilical vein catheter ran an unusual course (dots). **B.** Left renal vein and inferior vena cava (IVC) were detected after postmortem injection of a radiopaque dye from the umbilical vein catheter (dots).

The number of branches of portal vein in the portal tract was increased, and some of them demonstrated a significant muscular medial hypertrophy (Fig. 3B). Because of these changes, the portal vein was often difficult to distinguish from the hepatic artery. At times the dilated central vein herniated into the lobule (Fig. 3C). The lung:body weight ratio was 0.009, indicating pulmonary hypoplasia. The bronchioles and alveoli were patent, but their epithelium had been widely replaced by a hyaline membrane. The placenta was large and edematous. Microscopically, the villi were edematous too. There was no cardiac anomaly.

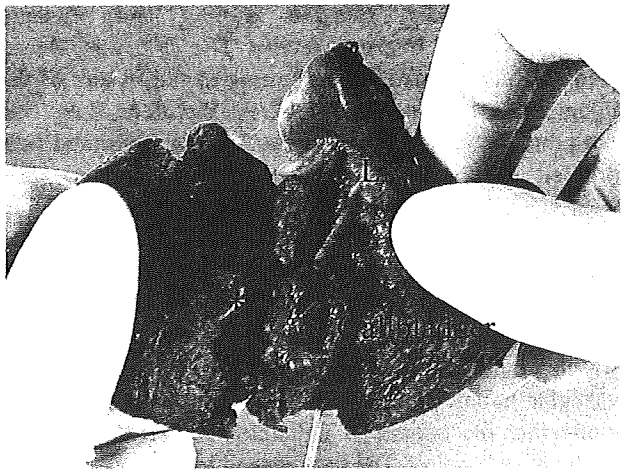

Figure 2. Macroscopic finding of liver. The ductus venosus was absent; it can normally be found in the area marked with an asterisk.

DISCUSSION

Agenesis of the DV has 2 main anatomic variations depending on whether umbilical venous connections are present or not [3,4]. In the 1st variation, with a left or a persistent right umbilical vein, the umbilical venous blood flow drains into the internal iliac vein, the IVC, or directly into the right atrium [3,5–7]. In this situation, the umbilical venous flow to the heart becomes uncontrolled, which may result in fetal congestive heart failure. In the 2nd variation, without these extrahepatic venous connections, the umbilical venous blood flow exclusively drains into the left portal vein, which may result in hyperperfusion of the liver sinusoids and may induce portal congestion and hydrops fetalis [4,8–10]. In our case, the baby had agenesis of the DV without extrahepatic umbilical venous

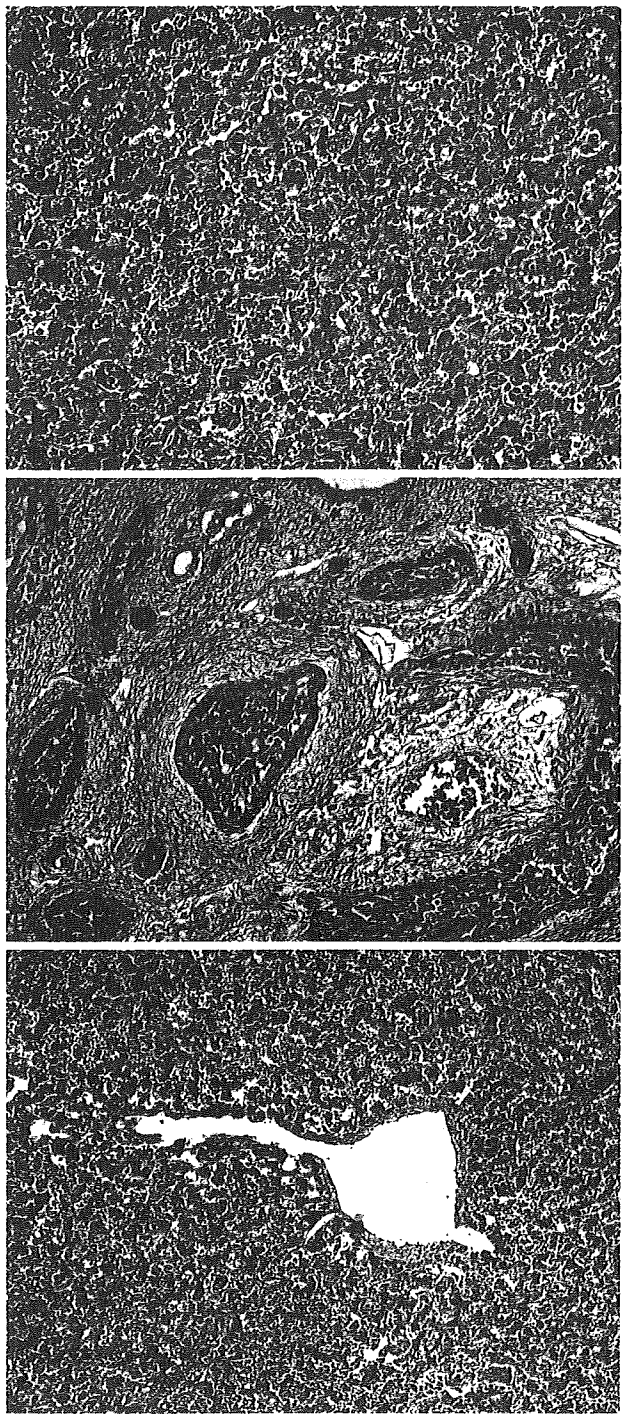

Figure 3. Microscopic findings of liver. **A.** The sinusoids and central vein of the liver were extensively and diffusely dilated. Extramedullary hematopoiesis was prominent. **B.** The portal vein had muscular medial hypertrophy. **C.** The dilated central vein herniated into the lobule.

drainage. He had portal congestion and collateral vessels due to portal hypertension that we could not initially recognize.

Agenesis of the DV without extrahepatic umbilical venous drainage is even rarer than that with it, but this condition has a favorable outcome in general [5,10]. In a recent study [11], Kiserud and colleagues detected 1 asymptomatic fetus with this anomaly among 202 normal pregnancies. Contratti and colleagues [5] and Gembruch and colleagues [10] reported 3 and 2 favorable cases, respectively. Moreover, in the fetal lamb, obstruction of the DV did not affect cerebral or regional organ blood supply because a dramatic increase of blood flow through the left lobe of the liver compensated for fetal circulation and oxygenation [12]. However, several cases [4,9] have been reported in postmortem series (Table 1). If the DV is absent, the oxygenated flow is disturbed. In addition, hyperperfusion of the sinusoids of the liver may induce prenatal portal hypertension [4]. Hepatic hyperperfusion, portal and umbilical vein hypertension, and placental edema could cause hepatic damage and impair fetal plasma protein synthesis and secretion. These findings are associated with an increased vulnerability to fetal hypoxia. In our case, the causes of hydrops fetalis were in all likelihood fetal hypoxia, portal hypertension, placental edema, and hypoproteinemia.

Additionally, the histological findings in the liver appear to be unique. There are few reports about hepatic histological findings with agenesis of the DV. Siven and colleagues [4] demonstrated 7 hepatic pathological findings in 8 cases. Six cases of pathological findings revealed diffuse sinusoidal dilatation, indicating hyperperfusion or congestion of the liver. Langman and colleagues [6] demonstrated agenesis of the DV with direct connection between the umbilical vein and the right atrium. This study revealed significant medial hypertrophy of the hepatic artery and a reduction in the number of the portal veins in the portal tract. The findings in our case are the same as those reported by Siven and colleagues, but our study presents findings not previously described: a significant medial hypertrophy of portal veins in addition to diffuse sinusoidal dilation, which is the same as noncirrhotic portal hypertension [13–15], especially hepatoportal arteriovenous fistula [13]. These findings might reveal a secondary change in the portal vein in response to increased portal pressure or long-standing portal hypertension.

In conclusion, we confirm the unfavorable outcome of some cases of agenesis of the DV without extrahepatic umbilical venous drainage and describe unique hepatic histological findings related to this condition. In addition, this report emphasizes the need for postmortem contrast angiograms of the umbilical vein drainage in cases of unexplained hydrops fetalis.

ACKNOWLEDGMENT

We thank Dr Jean-Claude Fouron (the Fetal Cardiology Unit, Division of Cardiology, Hospital Sainte-Justine, Montreal, QC, Canada) for his gracious review of this manuscript.

Table 1. Overview of reported and present postmortem cases with agenesis of the ductus venosus without extrahepatic umbilical venous drainage

Case	Sex	GA/age	Other malformation	Additional remarks	Hepatic pathology	Reference No.
1	Male	23 weeks	Pulmonary hypoplasia Hypoplastic heart	Hydrops fetalis Polyhydramnios	Enlarged liver Congestion of the sinusoids	4
2	Female	21 weeks	Pulmonary hypoplasia	Hydrops fetalis Polyhydramnios	Dilated sinusoids	4
3	Male	36 weeks/ at birth	Pulmonary hypoplasia	Hydrops fetalis	Abnormal lobulation of liver	4
			Hypoplastic heart Hygroma colli	Polyhydramnios	Extensive diffuse dilated sinusoids	
4	Female	39 weeks/ 11 hours	Signs of intrauterine asphyxia		Enlarged liver, dilated sinusoids Discrete steatosis	4
5	Male	36 weeks	Arthrogryposis multiplex congenita Severe ischemic lesions in the brain Hypospadia		?	4
6	Male	40 weeks/ 4 days	Partial situs inversus with asplenia		Midline liver	4
			Truncus arteriosus, PAVC, VSD, ASD bilateral IVC, fused adrenals		Extensive diffuse dilated sinusoids	
7	Male	40 weeks/ 2 hours	Partial situs ambiguous with asplenia		Abnormal lobulation of liver	4
			PA, PAVC, VSD, ASD Severe hypoplasia of pulmonary veins		Dilated sinusoids	
8	Female	40 weeks/ 15 days	HLHS, PLSVC		Enlarged and green liver Intrahepatic cholestasis	4
9	?	21 weeks	Pulmonary hyperplasia Hypoplastic heart	Hydrothorax	?	9
10	?	20 weeks		Hydrops fetalis	?	9
11	Male	36 weeks/ at birth	Pulmonary hypoplasia	Hydrops fetalis	?	9
			Hypoplastic heart, hygroma colli	Polyhydramnios		
12	Male	34 weeks/ at birth	Arthrogryposis multiplex congenita Microcephaly		?	9
13	Male	28 weeks/ 19 hours	Pulmonary hypoplasia	Hydrops fetalis	Congested liver	
Present Case					Extensive diffuse dilated sinusoids Muscular hypertrophy of portal veins Increased number of portal veins	

GA indicates gestational age; PAVC, persistent atrioventricular canal; VSD, ventricular septal defect; ASD, atrial septal defect; PA, pulmonary atresia; HLHS, hypoplastic left heart syndrome; PLSVC, persistent left superior vena cava.

REFERENCES

1. Rudolph CD, Rudolph AM. Fetal and postnatal hepatic vasculature and blood flow. In: Polin RA, Fox WW, eds. Fetal and Neonatal Physiology. Philadelphia: W.B. Saunders, 1998;1442–1449.
2. Kiserud T. The ductus venosus. Semin Perinatol 2001;25:11–20.
3. Jaeggi ET, Fouron J-C, Hornberger LK, et al. Agenesis of the ductus venosus that is associated with extrahepatic umbilical vein drainage: prenatal features and clinical outcome. Am J Obstet Gynecol 2002; 187:1031–1037.
4. Siven M, Ley D, Hangerstrand I, Svenningsen N. Agenesis of the ductus venosus and its correlation to hydrops fetalis and the fetal hepatic circulation: case reports and review of the literature. Pediatr Pathol Lab Med 1995;15:39–50.
5. Contratti G, Banzi C, Ghi T, Perolo A, Pilu G, Visentin A. Absence of the ductus venous: report of 10 new cases and review of the literature. Ultrasound Obstet Gynecol 2001;18:605–609.
6. Langman G, Wainwright H, Matthews L. Absence of the ductus venosus with direct connection between the umbilical vein and right atrium. Pediatr Dev Pathol 2001;4:298–303.

7. Sau A, Sharland G, Simpson J. Agenesis of the ductus venosus associated with direct umbilical venous return into heart-case series and review of literature. Prenat Diagn 2004;24:418–423.
8. MacMahon HE. The congenital absence of the ductus venosus. Lab Invest 1960;9:1227–1231.
9. Jorgensen C, Andolf E. Four cases of absent ductus venosus: three in combination with severe hydrops fetalis. Fetal Diagn Ther 1994;9:395–397.
10. Gembruch G, Baschat AA, Caliebe A, Gortner L. Prenatal diagnosis of ductus venosus agenesis: a report of two cases and review of the literature. Ultrasound Obstet Gynecol 1998;11:185–189.
11. Kiserud T, Rasmussen S, Skulstad S. Blood flow and the degree of shunting through the ductus venosus in the human fetus. Am J Obstet Gynecol 2000;182:147–153.
12. Rudolph CD, Meyer RL, Paulick RP, Rudolph AM. Effects of ductus venosus obstruction on liver and regional blood flows in the fetal lamb. Pediatr Res 1991;29:347–352.
13. Hashimoto E, Ludwig J, MacCarty RL, Dickson R, Krom RAF. Hepatoportal arteriovenous fistula: morphologic features studied after orthotopic liver transplantation. Hum Pathol 1989;20:707–709.
14. Nakanuma Y, Hoso M, Sasaki M, et al. Histopathology of the liver in non-cirrhotic portal hypertension of unknown aetiology. Histopathology 1995;28:195–204.
15. Abramowsky C, Romero R, Heffron T. Pathology of noncirrhotic portal hypertension: clinicopathologic study in pediatric patients. Pediatr Dev Pathol 2003;6:421–426.

Original Article

Gynecologic and Obstetric Investigation

Gynecol Obstet Invest 2009;67:137–144
DOI: 10.1159/000172805

Received: November 14, 2007
Accepted after revision: August 18, 2008
Published online: November 13, 2008

Change in Morphology and Oxytocin Receptor Expression in the Uterine Blood Vessels during the Involution Process

Tomoko Wakasa[a] Kenichi Wakasa[a] Masahiro Nakayama[b] Yuko Kuwae[b]
Keiko Matsuoka[b] Makoto Takeuchi[b] Noriyuki Suehara[c] Tadashi Kimura[d]

[a]Department of Diagnostic Pathology, Osaka City University Graduate School of Medicine, Departments of [b]Clinical Laboratory Medicine and Anatomic Pathology, and [c]Obstetrics, Osaka Medical Center and Research Institute for Maternal and Child Health, and [d] Department of Obstetrics and Gynecology, Osaka University Graduate School of Medicine, Osaka, Japan

Key Words
Involution · Uterine vessels · Oxytocin receptor · Intimal thickening

Abstract
Background: The histological changes in uterine blood vessels during pregnancy have been well investigated, but there have been few reports focusing on the changes in blood vessels during the involution process, especially within the first 24 h. We observed the process of uterine involution, focusing on the vessels of the resected uterus. ***Methods:*** Paraffin-embedded uterine samples from 15 patients who underwent hysterectomy because of severe cervical laceration and uterine rupture were examined. The time between delivery and hysterectomy ranged from 15 min to 456 h. The specimens were stained with hematoxylin-eosin, elastica-van Gieson and an antioxytocin receptor antibody. ***Results:*** Changes in the uterine vessels varied substantially based on their location. The intima in arteries of the endometrial side thickened within 5 h after delivery. On the serosal side, phlebosclerosis was demonstrated 6 weeks postpartum. Immunoreactivity for the oxytocin receptor (OTR) appeared in the muscular medias of arteries 5 h after delivery although it was not expressed before this period. ***Conclusion:*** Remodeling of uterine vessels involved thickening of the arterial intima and OTR expression in vessel walls during the first 5 h postpartum; the parameters normalized within 6 weeks. However, phlebosclerosis persisted for a long time on the serosal side.

Introduction

Histological changes in the uterine blood vessels during pregnancy have been investigated. To establish feto-maternal exchange, mononuclear extravillous trophoblasts invade through the uterine vessel wall, splaying apart and destroying muscular and elastic fibers [1, 2]. The uterine vessels are markedly dilated toward the second and third trimester of pregnancy, and finally the uteroplacental vessels keep approximately 500 ml of blood sequestrated at parturition. After delivery of the fetus, it is known that the uterus returns to the non-pregnant state; its weight decreases from approximately

KARGER
Fax +41 61 306 12 34
E-Mail karger@karger.ch
www.karger.com

0378–7346/09/0672–0137$26.00/0

Accessible online at:
www.karger.com/goi

Kenichi Wakasa
1-5-7 Asahimachi
Abeno-ku, Osaka City
Osaka 545-0051 (Japan)
Tel. +81 6 6645 2225, Fax +81 6 6646 3798, E-Mail wakasa@med.osaka-cu.ac.jp

Table 1. Cases

No.	Gravida	Para	Gestation, weeks	Age	Time after delivery	Mode of delivery	Complications
1	2	2	41	37	0 h 15 min	C/S +, induced	IUFD, rupture
2	3	3	39	31	0 h 30 min	C/S +, induced	IUFD, rupture (hydrocephaly)
3	7	3	40	35	5 h	vaginal +, spontaneous	cervical laceration
4	2	2	37	36	5 h	vaginal +, spontaneous	cervical laceration
5	4	3	38	30	5 h 5 min	vaginal +, spontaneous	cervical laceration
6	3	3	40	31	5 h 16 min	vaginal +, spontaneous	cervical laceration
7	6	6	37	36	5 h 40 min	vaginal +, spontaneous	rupture
8	4	4	40	34	6 h 22 min	vaginal +, spontaneous	cervical laceration
9	1	1	41	38	6 h 27 min	C/S +, induced	post-cesarean section laceration of uterine artery
10	2	2	38	34	6 h 48 min	elective C/S	post-cesarean section laceration of uterine artery
11	5	4	38	39	8 h	vaginal +, spontaneous	cervical laceration
12	2	2	40	29	9 h 40 min	elective C/S	post-cesarean section laceration of uterine artery
13	2	2	39	32	16 h	vaginal +, spontaneous	cervical laceration
14	2	2	29	32	110 h	C/S (PROM, Breech)	post-cesarean section laceration of uterine artery
15	5	3	40	31	19 days	vaginal +, spontaneous	cervical laceration
16	2	2	39	33	60 days	vaginal	CIN3
17	4	3	40	39	7 years	vaginal	CIN3
18	2	3	40	37	5 years	vaginal	CIN3
19	0	0		37			CIN3
20	0	0		38			CIN3
21	0	0		35			CIN3
22	0	0		30			CIN3

1,000 g immediately postpartum to 60 g by 6–8 weeks, i.e. involution of the uterus. During this period, uterine smooth muscles successively contract and constrict intermyometrial vessels, and large vessels at the placental site eventually thrombose. However, there have been few reports focusing on the morphological and functional changes in the uterine blood vessels during the involution process, especially in the first 24 h [3–5]. Therefore, the normal process of uterine vessel involution within the 24 h after parturition remains unclear.

In order to investigate uterine vascular involution, we retrospectively collected samples from hysterectomy due to massive hemorrhage caused by uterine rupture or severe cervical laceration. In patients with cervical laceration in whom hemorrhage could not be controlled after several attempts to suture the wound, hysterectomy was sometimes necessary shortly after delivery; uterine contractions were generally normal at the time of hysterectomy.

We focused not only on the morphology of uterine vessels, but also on their functional modulation. We examined elastin to visualize the structure of the internal elastic lamina (IEL), which determines vascular elasticity and tension opposing the expansile force of blood pressure.

Oxytocin plays a central role in inducing uterine smooth muscle contractions at parturition. In the rat, uterine artery smooth muscle sensitivity to oxytocin is attenuated during the course of pregnancy although its change during the postpartum period is unknown [6]. Postpartum, central oxytocin secretion is fully activated [7]. Breastfeeding apparently accelerates uterine involution via oxytocin stimulation [8]. However, the target tissue of oxytocin in the involuting uterus has not been fully elucidated.